

## General Comments:

The authors are to be commended for a manuscript and research that works toward answering a novel and important question in the study of precipitation processes. The leveraging of a suite of ground observations, combined with additional fields that must be obtained from NWP, works quite well to provide an analysis of this case. However, there are some important issues that need to be resolved before it should be accepted for publication. One of these issues, as I mention below, is fundamental to the entire purpose of this study, and therefore it is imperative that it be fully rectified.

We gratefully thank you for your review of our paper. We answer your line by line comments here below.

## Specific Comments:

P2,L1-16: This section needs a brief discussion of Atmospheric Rivers (ARs) and IVT, and a few citations about them. The first question I would like answered in here is: “are WCBs and ARs the same thing by definition? Is every WCB, and every location within a WCB, an AR? Is every AR a WCB?” I have seen both in the literature but do not know the difference.

A good start for citations would be Rutz et al. (2014):

<https://journals.ametsoc.org/doi/full/10.1175/MWR-D-13-00168.1>

The reason I suggest it as a good start is the usage and definition of IVT. The current study uses IVT, but I cannot find it defined anywhere. Also, since Rutz et al. define an AR as having  $250 \text{ kg m}^{-1} \text{ s}^{-1}$ , the authors should consider beginning their IVT contours at 250 in Fig. 2.

Thank you for this suggestion. There exists some work in the literature that specifically addresses the difference between ARs and WCBs (Knippertz et al. 2018, Dacre et al. 2019). The main difference is that WCBs are Lagrangian features (e.g. relative to an extra-tropical cyclone) defined as trajectories with an ascent greater than 600 hPa in 48 hours (Madonna et al. 2014). Atmospheric rivers are Eulerian features defined as 2D objects poleward of  $20^\circ$  latitude with  $\text{IWV} > 20 \text{ kg/m}^2$ ,  $\text{IVT} > 250 \text{ kg/m/s}$  and longer than 2000 km. They can be collocated, but often occur in isolation. WCBs are directly linked to baroclinicity and have a maximum of occurrence in winter in the storm tracks. There exists a secondary maximum of occurrence in strong orographic lifting regions (e.g. Andes, Himalaya), but otherwise the ascent is provided by large-scale baroclinic forcing. ARs are more frequent in summer and can be linked to non-cyclonic systems (e.g. monsoons). There is also no ascent in the definition.

Since we do not use the concept of ARs in this study, we think it is better not to introduce it explicitly. If we do insert it, it will be either too short and might confuse the reader or too long and out of the scope of this study. Instead we provided one reference (Dacre et al., 2019) that addresses the difference between WCBs and ARs, so that a reader not familiar with the difference can easily access it. This reference is added on P2,L1-3:

“Quasi-Lagrangian analyses of mid-latitude baroclinic storms showed the existence of three distinctive airstreams (Carlson, 1980): the dry intrusion, the cold conveyor belt (Harrold, 1973; Browning, 1990; Schultz, 2001) and the warm conveyor belt (WCB, Green et al., 1966; Harrold, 1973; Browning et al., 1973; Dacre et al., 2019).”

Concerning the definition of IVT, we added the reference of Rutz et al. 2014, so that the reader not familiar with this variable can find the definition. We think it is out of the scope of this study to explicitly write the equation, since it is not a central variable of this study and it would be difficult to argue why we explicit this variable and not others (e.g. potential vorticity).

Regarding the start of the IVT contours: we tried with the first contour at  $250 \text{ kg m}^{-1} \text{ s}^{-1}$ , but it decreases the overall readability of this figure (see Fig. 1 of this document) that already contains a lot of information. Since we focus on the most intense part of this atmospheric river, we decided to show only the values greater than  $500 \text{ kg}^{-1} \text{ m}^{-1} \text{ s}^{-1}$ . This information has been added in the caption of Fig. 2 of the paper, because it was missing.

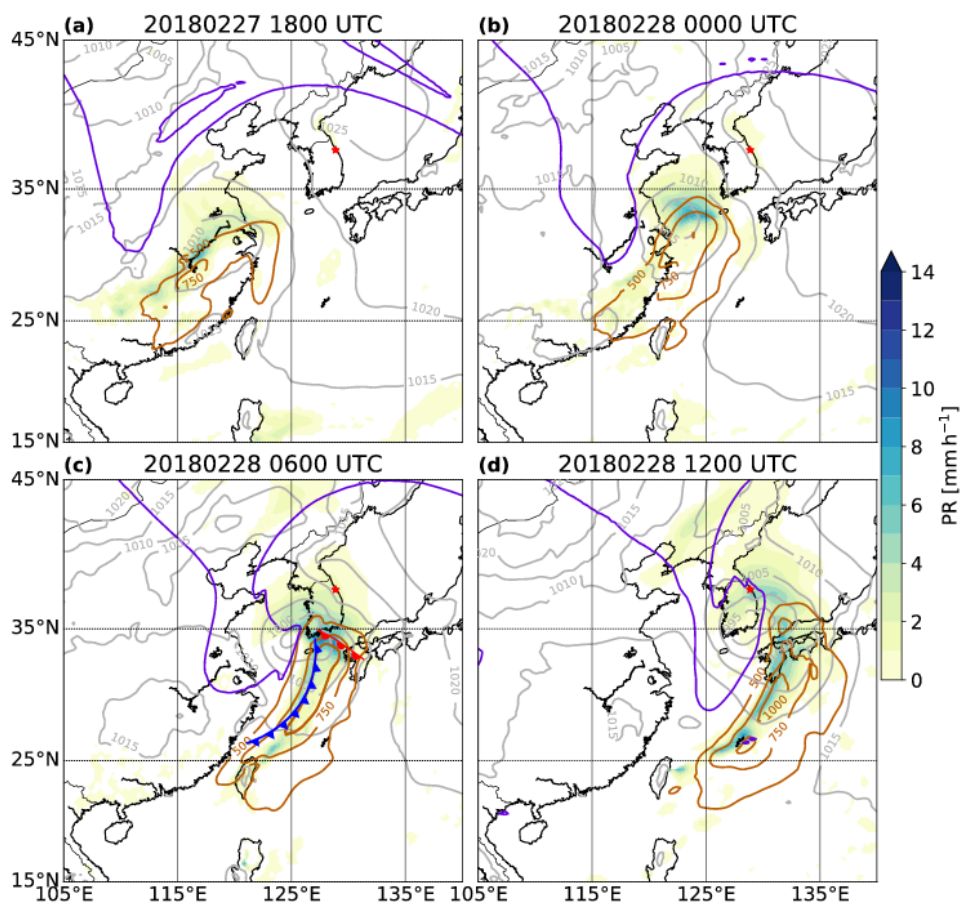
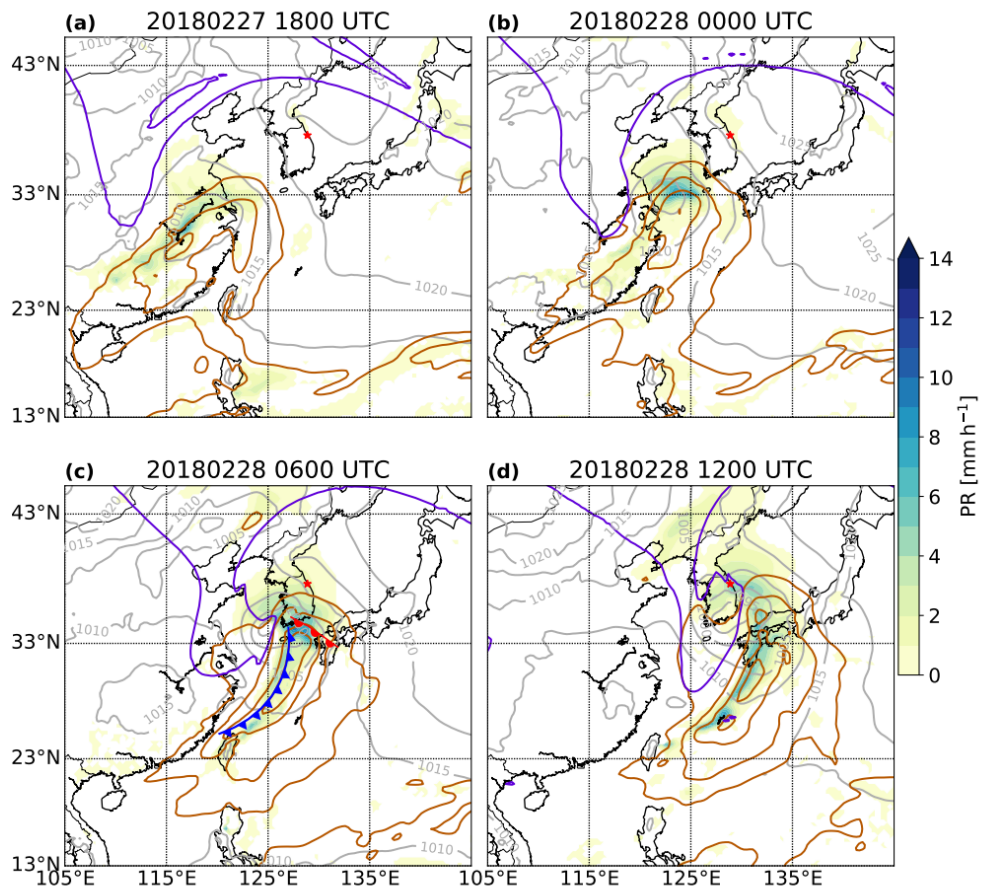


Figure 1: Same as Fig. 2 of the paper. (top) IVT starting at  $250 \text{ kg}^{-1} \text{ m}^{-1} \text{ s}^{-1}$ , (bottom) at  $500 \text{ kg} \text{ m}^{-1} \text{ s}^{-1}$

P2,L22-30: This portion of the review needs improvement. The general suggestion is that the authors need to provide the reader with the relevant background on dual-pol signatures in ice-phase and mixed phase situations, so that they are prepared to properly interpret the upcoming results they are about to encounter.

We totally agree with this comment. We added the suggested information and other dual-polarisation signatures that are relevant for the interpretation of the results in this study. The modified introduction can be found in the latest version of the manuscript and in the track changes document.

Specific suggestions:

a) The sentence “Grazioli et al. (2015) suggested that similar peaks in Kdp can result from secondary ice generation” is not representative of the Grazioli work. This should be changed to “Grazioli et al. (2015) suggested that similar peaks in Kdp can result from secondary ice generation or the riming of ice crystals with anisotropic shapes.”

Indeed, we changed it as suggested

b) There are three quotes in here (doi:10.15191/nwajom.2013.0119) that contain great info for the reader:

“The exact value of ZDR depends on the crystal density; solid ice particles such as hexagonal plates can have intrinsic ZDR values larger than 6 dB, in some cases even approaching 10 dB (e.g., Hogan et al. 2002), whereas the ZDR in dendrites generally remains below about 4–5 dB. However, because of particle wobbling, imperfect shapes, and a mixture of crystal types usually present in clouds, observed ZDR values in ice crystals usually do not exceed about 4–5 dB.”

“In contrast to the pristine ice crystals, large aggregates are observed to have very low ZDR (<0.5 dB). This is primarily attributable to their very low density (usually <0.2 g cm<sup>-3</sup>, compared to the density of solid ice of 0.92 g cm<sup>-3</sup>), which makes their exact shape less important from the radar’s perspective.”

“Additionally, increased fluttering of aggregates tends to keep ZDR quite low. Note that, because of their large sizes compared to pristine crystals, snow aggregates tend to have larger ZH values. Observations of ZH increasing towards the ground coincident with ZDR decreasing towards the ground are consistent with ongoing aggregation.” Please include this information (in a few sentences) in this section.

Thank you for these specific quotes. We included this information, together with an introduction of Kdp on P2,L25:

“For instance, differential reflectivity ZDR, defined as the logarithmic ratio between the reflectivity factor at horizontal and vertical polarisations (ZH–ZV in dB), is a measure of the reflectivity-weighted axis ratio of the targets (Kumjian, 2013). Oblate particles (e.g. raindrops, dendrites) have positive ZDR values, while prolate ones (e.g. vertically oriented ice in an electric field) exhibit negative ZDR values. ZDR also depends on the crystal density, but not on the number concentration. Therefore, large aggregates tend to have small ZDR (<0.5 dB, Kumjian 2013), primarily because they have a much lower density than solid ice, but also because they tend to be more spherical than pristine crystals. On the other hand, aggregates are much larger than crystals and tend to have higher ZH values. Consequently, decreasing ZDR together with increasing ZH towards the ground is a consistent sign of the aggregation process (Kumjian et al., 2014; Grazioli et al., 2015). Furthermore, the specific differential phase shift (Kdp in ° km<sup>-1</sup>), which is the range derivative of the total differential phase shift on propagation (i.e. phase difference between the horizontal and vertical polarisation waves), is related to the axis-ratio, the density, the number concentration and the size of the targets. Being a lower order moment than ZH, it is more influenced by the number concentration, such that a high number concentration of small oblate crystals can lead to an increase of KDP, while ZDR will barely be affected.”

Figure 2: the authors should consider decreasing the size of the geographic domain of the subplots, as it would be easier to see what is happening over Korea. I know there is a need to see the broader environment for cyclogenesis, etc., but I think a sizable reduction could be accomplished without losing any important large-scale details. Also, the locations of the labels of IVT contours could be made smaller and moved to locations that have fewer things drawn over the top of one-another. For example, the 1000 label in 2c is probably not needed – the reader can infer that.

We slightly decreased the domain, mostly we reduced the eastern extent, but we kept the longitude minimum to  $105^\circ$  to see the PV streamer approaching. We decreased the size of the IVT contour labels and removed the  $1000 \text{ kg}^{-1} \text{ m}^{-1} \text{ s}^{-1}$  label on panel c (see Fig. 1 of this document). In this way, we think the plot is more readable.

P6,L10: why not also “(iii) advection of liquid droplets from below to above freezing level”? This would technically become new SLW, correct?

Or change the sentence to “The increase on LWC is likely a result of...”, and the rest of the sentence would be correct.

Correct. We changed it to (P.6, L26): “The increase on LWC in supercooled conditions is likely a result of (i) condensation on the water droplets advected from below to above freezing level and (ii) nucleation of new droplets at subfreezing temperatures.”

P8,L3: Does the partial melting of the hydrometeors at low levels during this warmest period help explain the spike in brightness temperature? Does the presence of liquid on the MASC hydrometeors correlate at all with this spike?

It is a very good point that we indeed did not address. Yes, before 07:00 UTC the temperature is above freezing at MHS and the peaks in brightness temperature correlates with the onset of precipitation at 04:00 UTC and the maximum of precipitation rate at 06:00 UTC. The former is due to a large proportion of wet particles (>50% Fig. 2 in this document), because the temperature is of  $1^\circ\text{C}$  (Fig. 6e of the paper). The latter is due to strong precipitation at temperatures slightly above freezing ( $0.2^\circ\text{C}$ ) leading to partly melting hydrometeors ( $\sim 25\%$ ). So yes, for these two peaks there is a correlation with the presence of liquid water in the MASC images and it is consistent with the temperature above freezing. The peaks in brightness temperature after 07:00 UTC do not correlate with melting hydrometeors, but rather with updraughts. Since the temperature is below freezing after 07:00 UTC, it suggests the production of SLW. We modified this part in the manuscript as followed:

P8 L19:

“The maxima in brightness temperature observed when precipitation starts just before 04:00 UTC and at the peak at 06:00 UTC corresponding to the local maximum of precipitation rate (Fig. 5e), are probably due to partial melting of hydrometeors, since the near-surface temperature at MHS is above  $0^\circ\text{C}$ . The multiple peaks after 07:00 UTC (temperature below freezing), which are co-occurring with updraughts, suggest that the updraughts favour the production of SLW in addition to the SLW produced by the large-scale ascent in the WCB.”

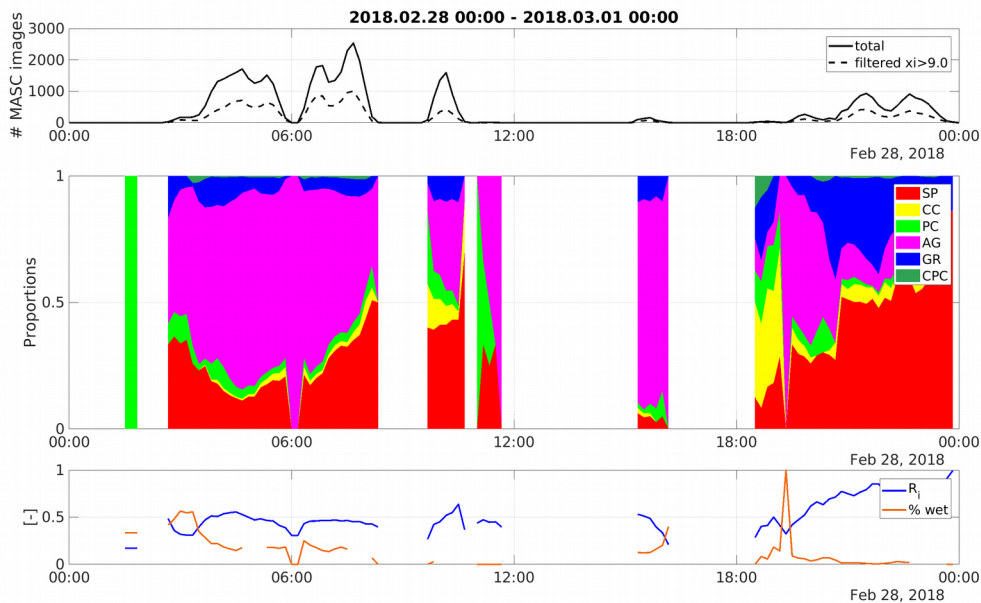


Figure 2: Time series of MASC data. (Top): number of images observed (dashed line those with a quality index greater than nine, see Praz et al. 2017). (Middle): hydrometeor classification. (Bottom): riming index (blue) and proportion of melting particles (orange).

Fig. 6d: please use a retrieval (perhaps from Kuchler et al. 2017) to obtain LW content and add it to 6d. The brightness temperature by itself is helpful, but does not quantify the LWC.

A reliable estimate of the LWC using the brightness temperature requires a large set of radiosondes data (Kuchler et al. 2017), which we do not have for this location. The software of the WProf radar provides an estimation of the LWP based on ERA-I data, but the algorithm has not been trained for South-Korea. Rather than showing a LWP which we are not confident in, we decided to show the brightness temperature, which is the main variable determining the LWP. Since we only use this information qualitatively (i.e. its relative evolution with time), we think it is better to show the raw measurement of brightness temperature. We added the following information in the manuscript: P.8 L.18: “The brightness temperature measured by the radiometer (Fig. 5d) is the primary variable used in estimations of the liquid water path (e.g. Kuchler et al., 2017). In this study, we will use the brightness temperature as an indicator of the temporal evolution of the total liquid water in the atmospheric column.”

P9,L1-3. As mentioned here, Fig. 8 indicates roughly the same fraction of graupel for this “vapour deposition” period as the fraction for Figs. 11 and 14. It also has the highest brightness temperature (and therefore LWC) of the entire study. It seems a bit odd to call this the “vapour

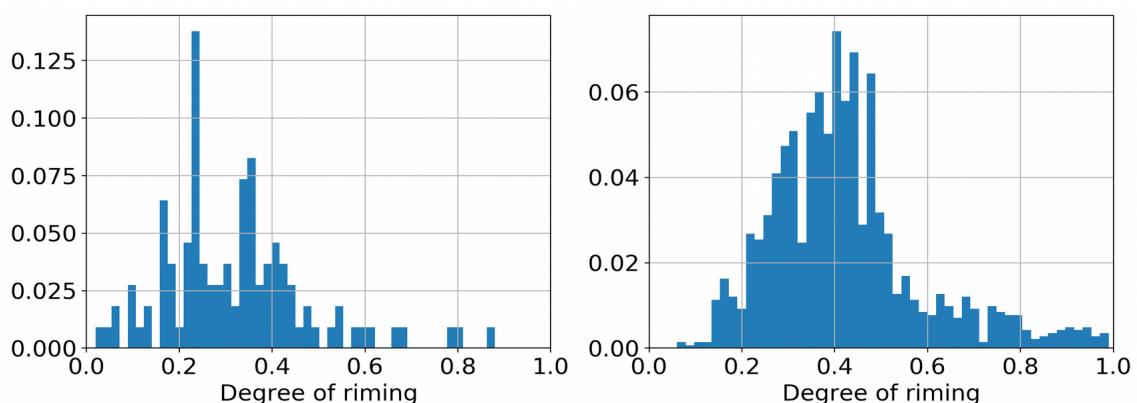


Figure 3: (left) Distribution of riming degree for 03-04 UTC without graupel nor small particles. (right) same for 06-08 UTC

deposition” period. I understand that the authors hypothesize that the riming happened below 2000 m, but that makes the claim of dominant vapor depositional growth during this period entirely dependent on the dual-pol hydrometeor classification scheme and inference from the sounding profile. It also undermines the main purpose of this study, as whatever mass was added by riming below 2000 m is quite important to the synoptic-microphysical connections that the authors are attempting to make in this paper. Where is this riming in the conceptual diagram (Fig. 16)? This is the most critical problem facing this manuscript.

Thank you for this comment, it is an important point in the manuscript that we had to address. The first point is that, even if the proportion of graupel is roughly the same for all periods, the number of particles and the precipitation intensity is much larger between 06-08 UTC. This means that the riming and aggregation processes taking place above 2000 m and which are directly linked to the WCB, are the most relevant for the precipitation accumulation. This is the most important message of the manuscript.

The second point is that, because they are close to the resolution limit, small particles tend to appear more spherical and brighter, two important factors in the classification of MASC images in Praz et al. (2017). This artificially increases the riming index of small particles.

The third point is that the graupel category includes only fully rimed particles. The aggregates category contain all aggregates from dry to almost fully rimed. The riming index distribution of Fig. 3 clearly shows that if one removes graupel and small particles, the period from 06 to 08 UTC is the most rimed and this contribution comes from rimed aggregates. The main message of this period is that the WCB is responsible for significant riming and aggregation which leads to large-rimmed aggregates and explain the large precipitation accumulation. The riming observed between 03-04 UTC is not contributing much to the overall precipitation accumulation.

We added the following on P.11 L.20:

“Note that while the previous period (Sec. 5.1) featured riming below 2000 m, the precipitation rate was much smaller than from 06:00 to 08:00 UTC (Fig. 5e) and hence this riming did not contribute significantly to the total precipitation accumulation. The important message here is that the flow conditions in the WCB promoted rapid precipitation growth by aggregation and riming above 2000 m and are thus responsible for the large precipitation accumulation between 06:00 to 08:00 UTC.”  
The riming in the conceptual model is represented by the blue liquid droplets accreting to the snowflakes (below 500 hPa).

Section 5.1. Would extending this period to 0500 UTC allow for a selection of MASC images without liquid water on them? The surface temperature cools a bit from 0400 to 0500. This would also make it the same 2-hour length (and sample size of radar scans) as the other two periods.

Yes, but the period 04-05 UTC is already dominated by aggregation leading to large particles, while 03-04 UTC is dominated by small particles. If we combine the two periods, the size distribution is closer to the period 06-08 UTC (see Fig. 2). The idea behind the section “microphysical analysis of periods of interest” is to analyse time periods that contain consistent processes associated with different phases of the WCB (i.e. outflow, ascent), not necessarily of the same duration. If we extend the period to 05:00 UTC, then we have a mix of small particles which grow by vapour deposition in the outflow of the WCB air masses and others which aggregated in the turbulent layer appearing after 04:00 UTC. This would be less relevant for our analysis.

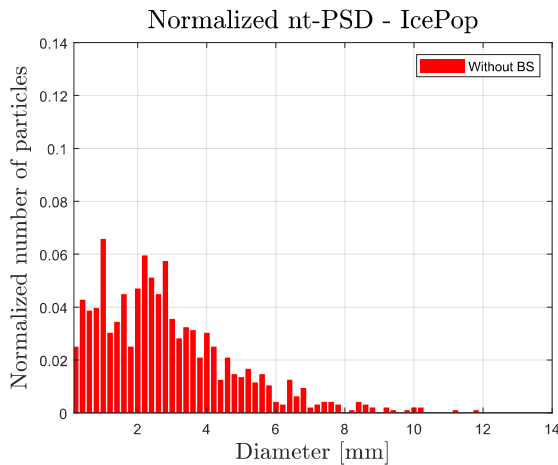


Figure 4: Normalised size distribution observed from 03:00 to 05:00 UTC.

P10,L5-7: It seems a bit optimistic to call any of those layers below 3000 m at 0600 potentially unstable. If those wiggles are averaged for even 200 m, there is a net increase in  $\theta_e$ . “Moist neutral” is probably more accurate. The flow has strengthened from period 5.1, and in Fig. 6b, from 789–2000 m, I instead see increased turbulence from the stronger flow potentially playing a role. The intense vertical motion in the 3000–6000 m layer in Fig. 6b most definitely cannot be attributed to anything but turbulence from the intense shear. I would focus on the shear-induced turbulence as the mechanism for the lifting here, with perhaps a brief mention that there could be a small contribution of buoyancy from the wiggles in the  $\theta_e$  line.

Good point. The shear-induced turbulence might indeed be the main reason for the observed updraughts. Figure 3 shows the gradient Richardson number ( $R_i$ ) from the three radio-soundings. Between 3000 and 6000 m,  $R_i$  is almost always below 1 for all three radio-soundings and sometimes below 0.25, which suggests indeed that the turbulence is shear-generated.

We removed the sentence P.10,L5:

“Moreover the layers of potential instability below 3000 m (Fig. 5a) indicate that instability can be released, if sufficient lifting is provided, for instance by the Kelvin-Helmholtz waves.”

and modified P11,L1:

“These sources of lifting together with the moist neutral layers below 3000 m (Fig. 6a) can lead to the observed strong updraughts (Fig. 5b), which promote aggregation by increasing the probability of collisions between particles.”

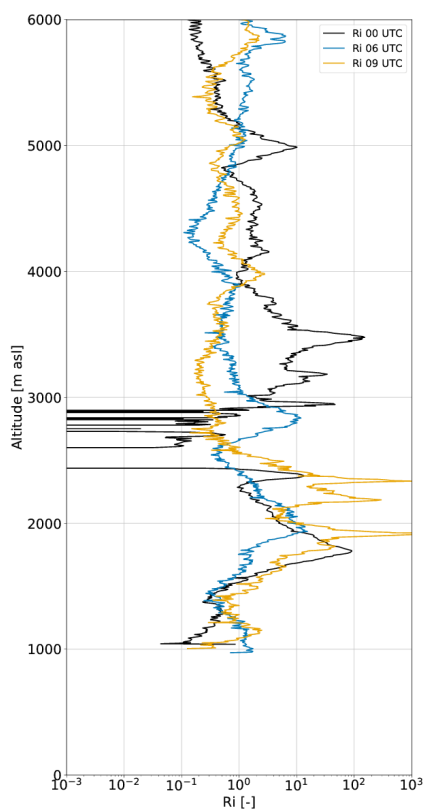


Figure 5: Gradient Richardson number computed from the radiosoundings

P10,L24-P11,L4: This section does not add much to the paper. The updraught being discussed is already the most salient feature in Fig. 6b, and Figs. 12 and 13 do not provide much in the way of information that cannot be gleaned from Figs. 6a,b. I would suggest dramatically shortening this section.

We decided to remove Fig. 13 and its corresponding discussion (P. 11, L 5-9), because indeed it does not add much to the paper. However we decided to keep Fig. 12 and its interpretation, because we think that the discussion on the increase of the spectral width during the updraught is relevant to show that the updraughts are responsible for the increases in turbulence and hence aggregation. The fact that in Fig. 12b the spectral reflectivity increases with a decrease in Doppler velocity further supports this hypothesis of strong aggregation in the turbulent layer and fall of the hydrometeors once they grew big enough to compensate for the updraught. The subsequent discussion on the timing of the strong updraught and the increase in precipitation intensity is relevant for our hypothesis that the embedded convection is responsible for the strongest precipitation observed.

P11,L2-4: Why does this suggest that convection is responsible? There is no substantial evidence to support that conclusion. There is no instability anywhere near this level in the 0600 sounding, and why could it not be a particularly strong KH billow?

The cause of this updraught cell with a vertical extent of 2000 m cannot be directly assessed with the radio-soundings at 06:00 and 08:00 UTC. However it is very consistent with embedded convection within warm frontal cloud as observed by Hogan et al. 2002, Keppas et al. 2018 and Oertel et al. 2019. Hogan et al. 2002 showed that Kelvin-Helmholtz instability can generate embedded convection. In addition the radio-sounding at 06:00 UTC shows a strong shear just below



4000 m exactly where the strong updraught cell starts. This probably generated the updraught cell, which continue to propagate upwards. Just below 6000 m, where the updraught cell stops, there is a stable layer of about 100 m, which might have stopped the updraughts.

We did not find any case in the literature of such vertically extended KH billows. In addition the term embedded convection is often used without a specific mention of static instability (Hogan et al. 2002, Keppas et al. 2018). However, since we cannot evidence the presence of convective instability, we decided to replace the occurrences of “embedded convection” that were referring specifically to this case with embedded updraught. We added a sentence in this direction on P.8, L14:

“While the cause of the updraughts we observe might be different than those mentioned in Hogan et al. (2002), Keppas et al. (2018), Oertel et al. (2019a), the consequence on precipitation growth processes is consistent with what we observe in this study.”

P11,L3: It would be more convincing if the “intense riming” were obvious in the MASC image (Fig. 11). If anything, the riming in period 5.3 (Fig. 14) seems more intense to my eye, but it is difficult to assess with much certainty from the images. Was there any sort of disdrometer, especially a PARSIVEL, available at the site? If so, the density of the hydrometeors could be calculated from it. If the density were compared for particles of similar size, this would provide a more precise quantification of the degree of riming than the MASC.

According to Battaglia et al. 2010, fall velocity measurements of solid hydrometeors from PARSIVEL lead to an underestimation of up to 20%. Instead, the MASC can provide the riming index together with fall velocity measurements, which we are more confident on the accuracy, since it was installed in a DFIR. From Fig. 6, it is clear that the period 06-08 UTC has larger riming index and, despite lower quartiles, has larger maximum fall-speeds than the period 03-04 UTC.

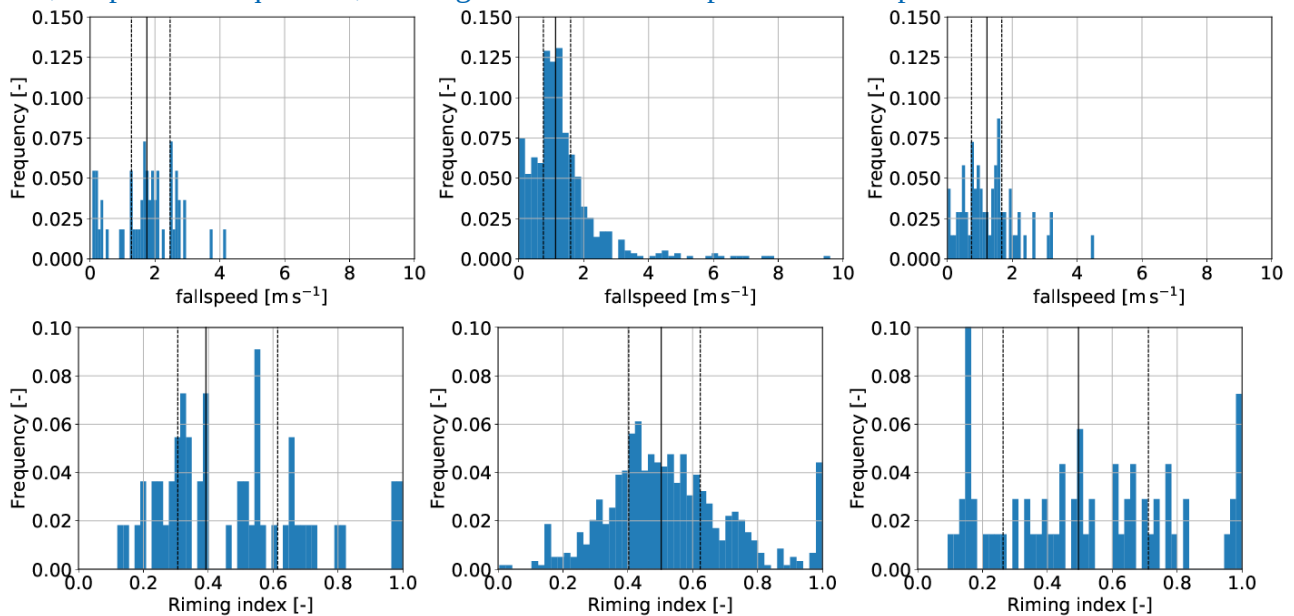


Figure 6: (Top) Distribution of fallspeeds for (left) 03-04 UTC, (middle) 06-08 UTC, (right) 09-11 UTC. (Bottom): same for riming index. The dashed lines shows the 25<sup>th</sup> and 75<sup>th</sup> percentiles of the distribution, the solid line shows the median.

P11,L13: “there are substantially more crystals and graupel particles than during other periods”.

This is true of the crystals, but the graupel concentrations are 9.1%, 8%, and 9.2% for the respective periods. I’d say that’s about the same amount of graupel for each period.

True, we removed “and graupel particles” from this sentence. This is related to the limitations of the classification of small particles in MASC images (see above).

P12,L11-12: The authors attribute the change from low Kdp in period 5.1 to high Kdp in 5.2 and 5.3 to the appearance of secondary ice. However, it seems there are two other possibilities. (1) as the authors mention, the number concentration of crystals is low in 5.1, and the greater concentrations of oblate targets/more intense precipitation in 5.2 and 5.3 are responsible for the increased Kdp. (2) The crystals in 5.1 are lightly rimed, and the onset of heavier riming in 5.2 and 5.3 is responsible for the increased Kdp. Please discuss this somewhere, and explain why either or both of those hypotheses can be ruled out.

Thank you for this comment. We did not properly address the effect of precipitation intensity and increase in concentration in the Kdp signature. We hypothesise that the increase in Kdp compared to period 5.1 is primarily due to the increase in precipitation intensity, but that the fact that it is collocated with aggregation and riming needs another mechanism to produce a high number concentration of oblate particles. We added this explanation on P10,L22:

“Note that the higher Kdp values compared to the period 03:00-04:00 UTC is primarily due to the increase in precipitation intensity, but the fact that Kdp increases below the onset of aggregation cannot be explained by precipitation intensity only, since aggregation decreases the number concentration and the oblateness of the particles. Riming initially increases Kdp by first filling cavities and hence increasing the density of particles, but later on leads to a decrease in Kdp as the rime mass will smooth the particles' shape. There has to be a mechanism which produces a high number concentration of oblate particles to explain an increase in Kdp in a layer dominated by aggregation and riming.”

#### **Technical Corrections:**

Multiple Locations: the phrase “associated to” would be more correctly written as “associated with”.

Thank you, we corrected it.

Multiple Locations: is there a “Wernli” and a “Werni” citation, or is this a typo? Correct throughout the manuscript.

We corrected this typo.

P5,L27: change “more and more” to “increasingly”

We corrected it.

Fig 5. Can the authors plot wind barbs somewhere on here? It helps to visualize the shear layers.

We think it would decrease the visibility of the figure to add three (one per sounding) wind profiles with wind barbs. We could replace the wind speed and direction plots by wind barbs only, but we prefer to keep them, as it allows a direct reading of speed and direction values.

Fig. 6. Please enlarge the figure slightly if possible. The details in 6c are the most difficult to see.

We increased the width of this figure.

Fig. 6c: please add a colorbar with labels for the hydrometeor information, instead of listing it in the caption – I don't know what “cerise” is, and there appear to be more colors than you describe in the caption. Please also provide a citation for the hydrometeor classification algorithm that is used.

We added the legend and changed the colours: now rimed particles are in red, which is easier to see. We also added the reference of the classification algorithm in the caption. The updated figure and its caption can be found at the end of this document.

Figs. 7, 9, 15: Please add a 5th subplot of temperature. Shouldn't the line corresponding to the lower limit of the WCB change for each period?

We added the temperature subplot. We also corrected the line corresponding to the lower limit of the WCB. The updated figures and their captions can be found at the end of this document.

Fig. 15. Caption should instead say "Same as Fig. 7", correct?

Correct, thank you for pointing that. We corrected it.

## References

Dacre, H. F., Martínez-Alvarado, O., and Mbengue, C. O.: Linking Atmospheric Rivers and Warm Conveyor Belt Airflows, *Journal of Hydrometeorology*, 20, 1183–1196, <https://doi.org/10.1175/jhm-d-18-0175.1>, 2019.

Hogan, R. J., Field, P. R., Illingworth, a. J., Cotton, R. J., and Choullarton, T. W.: Properties of embedded convection in warm- frontal mixed-phase cloud from aircraft and polarimetric radar, *Quarterly Journal of the Royal Meteorological Society*, 128, 451–476, <https://doi.org/10.1256/003590002321042054>, <http://dx.doi.org/10.1256/003590002321042054>, 2002.

Keppas, S. C., Crosier, J., Choullarton, T. W., and Bower, K. N.: Microphysical properties and radar polarimetric features within a warm front, *Monthly Weather Review*, 146, 2003–2022, <https://doi.org/10.1175/MWR-D-18-0056.1>, 2018. Knippertz, P., Wernli, H., Binder, H., Böttcher, M., Joos, H., Madonna, E., Pante, G.,

and Sprenger, M.: The Relationship between Warm Conveyor Belts, Tropical Moisture Exports and Atmospheric Rivers, 20th EGU General Assembly, EGU2018, Proceedings from the conference held 4-13 April, 2018 in Vienna, Austria, p.4362, 20, 4362, URL <https://presentations.copernicus.org/EGU2018-4362/presentation.pdf>, 2018.

Madonna, E., Wernli, H., Joos, H., and Martius, O.: Warm conveyor belts in the ERA-Interim Dataset (1979-2010). Part I: Climatology and potential vorticity evolution, *Journal of Climate*, 27, 3–26, <https://doi.org/10.1175/JCLI-D-12-00720.1>, 2014.